



Marine Heatwaves Variability and Trends in the Patagonian Shelf

Ana L. Delgado^{1,2}, Vincent Combes^{1,3}, Gotzon Basterretxea¹

¹Institut Mediterrani d'Estudis Avançats (IMEDEA, CSIC-UIB), Esporles, 07190, Spain.

⁵²Instituto Argentino de Oceanografía (IADO-CONICET-UNS), Bahía Blanca, 8000, Argentina.

³Departamento de Física, Universitat de les Illes Balears, Palma de Mallorca, 07122, Spain.

Correspondence to: Ana L. Delgado (aldelgado@imedea.uib-csic.es) and Vincent Combes (vcombes@imedea.uib-csic.es)

Abstract. Marine heatwaves (MHWs), defined as periods of persistently anomalous warm ocean temperatures, have doubled in frequency worldwide in recent decades and are becoming longer, more intense, and increasingly disruptive to marine ecosystems. In this study, we use 42 years of satellite-derived daily sea surface temperature (SST) data to characterize the frequency, intensity, duration, and long-term trends of MHWs in the Patagonian Shelf (PS). On average, the PS experiences 2.5 events year⁻¹, with a cumulative duration of 20 to 30 days annually and intensities ranging from 0.5°C to 2.5°C. The northern PS shows clear evidence of an increase in MHW days (+5-10 days decade⁻¹), whereas no significant trends are observed in the southern region (i.e., south of 48°S). Across the PS, MHW intensity exhibits a modest downward trend of roughly -0.2 °C decade⁻¹. Part of MHW variability is attributable to the El Niño Southern Oscillation. In particular, the highest annual total of marine heat-wave days was observed during the strong La Niña event of 1998 and both MHW intensity and duration tend to increase during La Niña episodes, with MHW intensity showing a more consistent association with La Niña conditions. We also examine the influence of the MHW detection method, fixed versus moving climatology, on MHW statistics. We find that over the PS, the methodological impact on key MHW metrics is minimal, especially when compared to the deep ocean, where substantial background SST trends amplify methodological differences. These findings underscore the necessity of region-specific assessments of MHWs to elucidate their future evolution and pace of change within the broader context of climate change.

25

30



1 Introduction

Marine heatwaves (MHWs) are defined as prolonged periods during which sea surface temperatures (SSTs) are abnormally high, typically surpassing a threshold based on the statistical characteristics of the local climatological SST distribution (Hobday et al., 2016). The impacts of MHWs are extensive, influencing both physical and biological processes in the ocean, 35 and they have been increasingly recognized as a key driver of ecosystem change in the context of the contemporary climate regime (Smale et al., 2019; Suryan et al., 2021). Physical consequences of their presence, such as increased water column stratification, reduced dissolved oxygen levels, and hindered sea ice formation, have been reported in recent times (e.g., Brauko et al., 2020; Hu et al., 2020; Carvalho et al., 2021). However, MHWs are not just a physical oceanographic phenomenon. They are associated with significant disruptions to ecosystems, including changes in phytoplankton community structure, coral 40 bleaching, altered migration patterns, and mass mortality events among various marine species, including mammals (Cavole et al., 2016; Genevier et al., 2019; Smale et al., 2019). The effects of these changes are especially pronounced in coastal and benthic environments where organisms cannot escape the altered ocean temperature conditions. Additionally, MHWs can result in broader systemic impacts, such as declines in fisheries, alterations in atmospheric circulation, and disturbances in air-sea carbon fluxes (e.g., Oliver et al., 2017; Cheung and Frölicher, 2020; Mignot et al., 2022).

45 Over the past century, both the frequency and duration of MHWs have increased globally, with the total annual number of MHW days rising by more than 50%. This trend is largely attributed to persistent upper-ocean warming, which is driven by anthropogenic climate change (Oliver et al., 2018; 2019; 2021). Climate model projections indicate that the frequency, duration, and intensity of MHWs are likely to intensify significantly under future warming scenarios. It is estimated that the 50 number of MHW days could increase by an order of magnitude by the end of the 21st century, particularly in coastal regions (Frölicher et al., 2018; IPCC, 2021). However, anthropogenic forcing is not the only contributor to global MHW variability. Internal modes of climate variability, such as the El Niño-Southern Oscillation (ENSO), have also been recognized as critical drivers influencing MHW occurrence on both regional and global scales (Heidemann and Ribbe, 2019; Liu et al., 2022; Gregory et al., 2024).

55 Over the Southwestern Atlantic Ocean, a recent study by Artana et al. (2024) highlights a relationship between MHWs' key metrics, such as intensity and duration, and ENSO events. However, the incidence of climate forcing at regional scales the incidence of climate forcing exhibits significant regional variability due to the combined effects of coastal topography, bathymetric complexity, freshwater inputs from rivers, and other localized factors (e.g., Stott et al., 2010; Xie et al., 2015; Kitchel et al., 2022). These features enhance biological productivity, making the Patagonian Shelf (PS) not only one of the 60 most biologically productive regions globally but also a major carbon sink that supports one of the world's most important fisheries. Within this framework, extreme thermal anomalies, whether locally generated or advected from adjacent regions, have the potential to induce substantial perturbations in ecosystem structure and function, with far-reaching environmental and socioeconomic consequences.



In this study, we assess and characterize the MHWs in the PS region. The paper is structured as follows: first, we perform a comparison of MHWs detection methodologies and different datasets. Then, we provide a regional characterization of MHWs 65 in the PS, examining their mean and seasonal distribution, long-term trends, and interannual variability, with particular attention to their relationship with ENSO events.

2 Materials and Methods

2.1 Regional Setting

The Patagonian Shelf, on the western boundary of the SWA, constitutes an elongated (55°S – 35°S) and relatively shallow 70 plateau with a variable width (100-400 km; Fig. 1a). Regional oceanography in open waters is characterized by significant mesoscale activity driven by the interaction of two sharply contrasting western boundary currents: the Brazil Current (BC) and the Malvinas Current (MC, Matano & Philander, 1993; Olson et al., 1988). These currents converge near 38°S, forming the highly dynamic Brazil/Malvinas Confluence (BMC), a region characterized by the persistent generation of warm and cold core eddies and filaments (Gordon and Greengrove, 1986; Gordon, 1989), and eddy kinetic energy values exceeding 2000 cm² s⁻² 75 (Fig. 1c). The MC, originating from the Antarctic Circumpolar Current (ACC), flows northward along the shelf-break carrying cold fresh waters, while the BC transports warm, salty waters southward (Matano & Philander, 1993, Fig. 1b). The spatial distribution of surface EKE maxima forms a distinctive C-shape surrounding a central region of relatively low EKE values in the basin's center (Fig. 1a). This central minimum is associated with a topography-driven oceanographic feature known as the Zapiola Anticyclone (ZA).

80 Within the PS, Sub-Antarctic cold waters enter through the southern boundary and mix with freshwaters inputs from the Magellan Strait and several rivers (Dai and Trenberth, 2002). The mean circulation is directed northeastward, driven by atmospheric forcing (Rivas, 1997; Palma and Matano, 2004) and cross-shore pressure gradients induced over the outer shelf by the Malvinas Current (Matano et al., 2010). Mean SSTs along the shelf present clear latitudinal variation, ranging from 6°C in the southern area to 17°C in the Río de la Plata mouth (Fig. 1b). The SWA exhibits contrasting SST trends (Fig. 1c). North 85 of 48-50°S, at the Brazil/Malvinas Confluence, the surface ocean is warming at a rate of 0.4°C decade⁻¹ as a result of the poleward migration of the BMC (Artana et al., 2019; Franco et al., 2020), whereas to the south, the temperature is slightly decreasing at a rate of -0.1°C decade⁻¹ (Delgado et al., 2023).

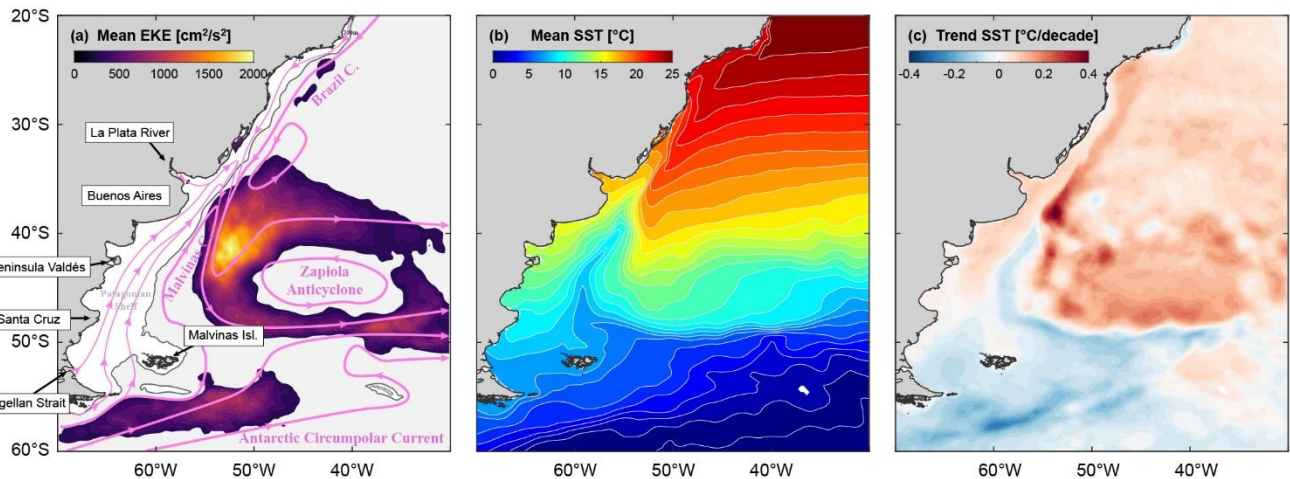


Figure 1: General oceanographic characteristics of the SWA and PS. (a) Schematic circulation of the study area and mean Eddy Kinetic Energy (EKE) in $\text{cm}^2 \text{s}^{-2}$; (b) Mean Sea Surface Temperature (SST, $^{\circ}\text{C}$) and (c) SST trend ($^{\circ}\text{C decade}^{-1}$).

2.2 SST datasets

We base our analysis on satellite-derived SST data provided by the European Space Agency's Climate Change Initiative Program (ESACCI), which is dedicated to extending, stabilizing, and enhancing the accuracy of climate data records for SST. The 42-year climate database provides daily SST at 0.05° resolution, from 1980 to 2021, obtained from twenty infrared and two microwave radiometers (Embry et al., 2024). This database was selected for its stability, designed specifically for climatological studies (i.e., Boisséson and Balmaseda, 2024; Konsta et al., 2025). However, to assess the influence of database selection on the characterization of MHWs, we conducted a comparative analysis of ESACCI against three alternative data sources: OSTIA-SST, NOAA-SST, and ERA-SST.

- OSTIA-SST is the Operational Sea Surface Temperature and Ice Analysis (OSTIA) dataset, produced by the UK Met Office and provided by IFREMER PU. It combines satellite data from the GHRSST project along with in situ observations to assess SST from 1981 (Good et al., 2020).
- NOAA-SST dataset corresponds to the daily Optimum Interpolation Sea Surface Temperature product (OISST V2.1) provided by the National Oceanic and Atmospheric Administration. This dataset offers a globally gridded, gap-filled field of sea surface temperature, derived primarily from remotely sensed observations acquired by the Advanced Very High-Resolution Radiometer (AVHRR). It features a spatial resolution of 0.25° and extends from 1981 to the present (Huang et al., 2021).
- ERA5-SST refers to the fifth-generation reanalysis of SST by ECMWF, based on in-situ data assimilation, providing a comprehensive record from 1940 onward (Hersbach et al., 2023).



2.3 MHW detection methodologies

The standard approach among marine scientists follows the definition by Hobday et al. (2016): Days with temperatures warmer than the 90th percentile based on a daily climatology baseline are considered MHW days. Only prolonged events lasting at least 5 consecutive days are further considered, with interruptions of up to two days being allowed.

In this study, we first consider a “Fixed Baseline” (FB; similar to Hobday et al. (2016)) daily climatology computed over the period 1982-2021 (40 years) to calculate key MHW metrics such as frequency, number of MHW days, and intensity. However, the influence of ongoing ocean warming trends on MHWs detection has sparked a debate on the optimal criteria for defining the baseline reference thresholds. If long-term temperature trends are not accounted for, MHW occurrence and duration may be overestimated (Oliver, 2019). The current discussion centers on whether a fixed or a moving baseline offers differing perspectives on MHW statistics (Oliver, 2019). However, while these approaches often yield different results, the choice of method should ideally be context-dependent and consider the adaptive capacity of regional ecosystems (Holbrook et al., 2019). We therefore additionally compute the MHW statistics using a “Moving Baseline” (MB), which updates the daily climatology annually using the last 20 years. Finally, the sensitivity of MHW statistics to the length of the baseline period (from 5 to 40 years) is also assessed.

2.4 Climate indices

El Niño Southern Oscillation (ENSO) is one of the strongest interannual climate variability phenomena that severely disrupts global atmospheric patterns (McPhaden et al., 2006). It is characterized by temporal variations of 2 to 4 years oscillations between warm (El Niño) and cool (La Niña) phases (Webster and Palmer, 1997). In the PS, ENSO has been linked to an increase in the frequency and/or intensity of climate-driven ocean variability events (e.g., Cai et al., 2020; Risaro et al., 2022). Specifically, Artana et al. (2024) reported a strong correlation between MHWs and ENSO events in the SWA. In this context, the interannual variability in the number of days and intensity was related to ENSO phases. To characterize these phases, we use the Southern Oscillation Index (SOI), which is based on the observed sea level pressure differences between Tahiti and Darwin, Australia (Climate Prediction Center, NOAA). The negative phase of SOI corresponds to El Niño years, whereas the positive phases of SOI correspond to La Niña years.

3 Results and discussion

3.1 Comparative baseline climatology criterion and database selection

3.1.1 Effect of the MHW detection methods on the MHW metrics

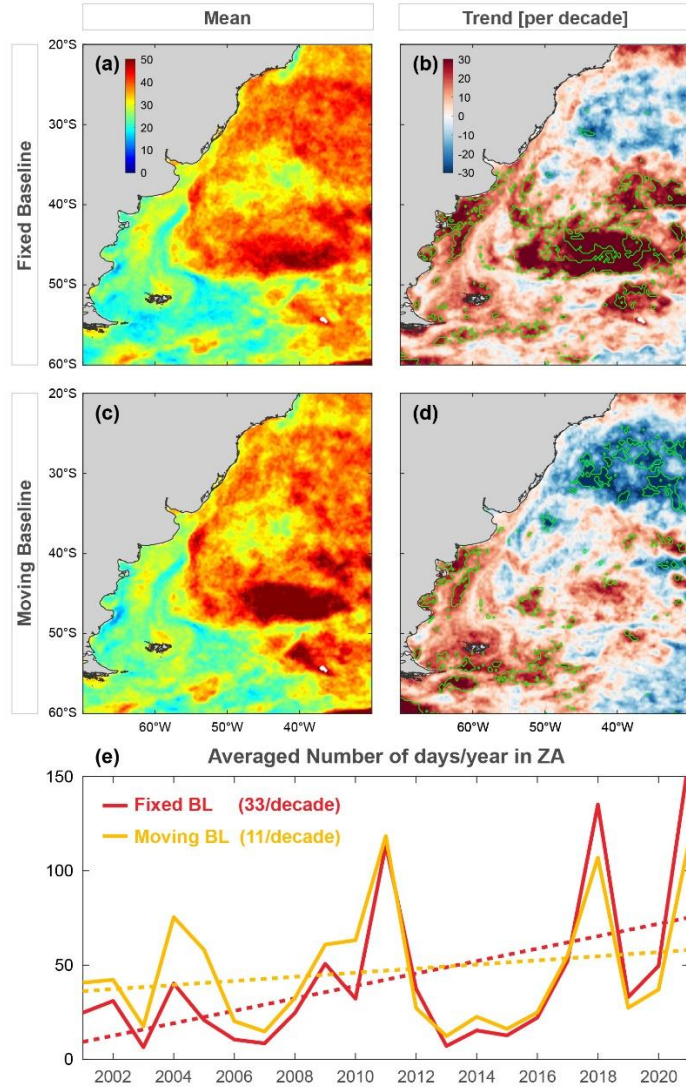
Long-term changes in background climate variability can substantially influence the detection and characterization of extreme events, particularly when static climatological baselines are employed, as these may fail to represent contemporary oceanic states. Consequently, outdated reference periods can lead to misrepresentations of the probability of exceeding or falling below



threshold values. This issue is particularly evident in climate model projections of SST. For instance, Roselló et al. (2023) show that, in a warming Mediterranean Sea, a fixed baseline results in saturation of MHW days, reaching 365 days year⁻¹ by 140 the end of the 21st century under the SSP5-8.5 scenario, compared to approximately 100 days year⁻¹ in the past decade.

Figure 2 reveals the differences in applying the FB and the MB method on the SWA region. Differences are most pronounced in the open ocean and where SST trends are stronger (see Fig. 1c), particularly over the Zapiola Anticyclone (ZA). Using the fixed baseline method, the trend in MHWs days shows values 3-fold higher than with the moving baseline method for the 145 period 2001-2021, with 33 and 11 MHWs/year/decade, respectively (Fig. 2e). Similarly, the weak negative MHW days trend east of the Brazil Current using a fixed baseline becomes statistically significant using a moving baseline strategy. Over the Patagonian shelf, differences between both methods are weaker (Fig. 2), and the impact on the long-term trends is mostly negligible.

The length of the baseline period also has a strong influence on marine heatwave (MHW) statistics. Although somewhat subjective, there is general agreement that the baseline period should be at least 30 years. To illustrate this sensitivity, we 150 examine how different baseline lengths affect MHW statistics in the ZA region, where sea surface temperature (SST) trends are significant (Fig. 3a). Figure 3b illustrates the number of MHW days per year calculated using different baseline lengths ranging from 5 to 40 years (Fixed Baseline method starting on 1982). When using a 30-year baseline climatology (1982–2011), the average number of MHW days is approximately 45 per year. We find that the highest number of MHW days occur 155 with a 16-year baseline climatology (~75 days/year), while the lowest (~30 days/year) is observed using a 40-year baseline climatology. Spatially, the length of the baseline climatology associated with the maximum number of MHW days is shown in Fig. A1 and closely resembles the map of SST trends (Fig. 1c). This preliminary analysis highlights the need for further investigation into the influence of baseline length, especially in regions with strong decadal SST variability, such as the northwest Pacific, where the Pacific Decadal Oscillation plays a major role. The sensitivity of MHW trends to baseline length is further illustrated in Fig. 3c.



160

165

Figure 2: Comparison of two baseline methodologies (FB and MB) for the detection of MHWs in the SWA. (a) Mean number of days by year of MHWs and (b) trend of the number of days by decade of MHWs using the fixed baseline approach. (c) Mean number of days by year of MHWs and (d) trend of number of days by decade of MHWs using the moving baseline approach. (e) Comparison of both methodologies on the interannual variability of the mean number of days in the Zapiola Anticyclone. Delimited green areas stand for a statistically significant trend ($p < 0.05$).

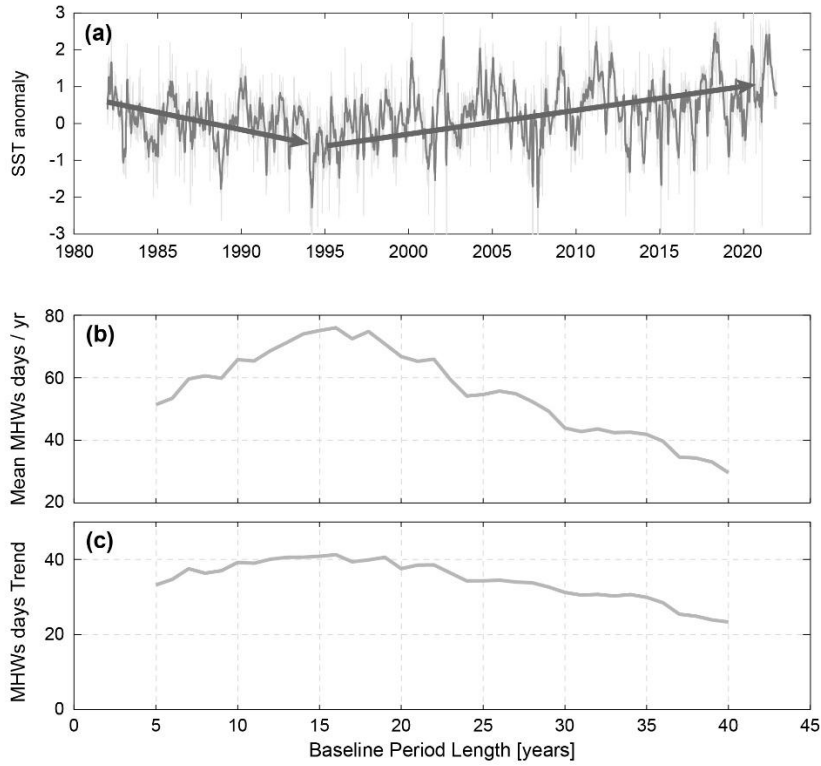


Figure 3: (a) SST anomaly (°C) in the Zapiola anticyclone. (b) Number of MHW days year⁻¹ (averaged over 1982-2021) for different baseline period lengths (in years) ranging from 5 to 40 years (starting in 1982). (c) same as (b) for the trend in MHWs days [#days yr⁻¹ decade⁻¹].

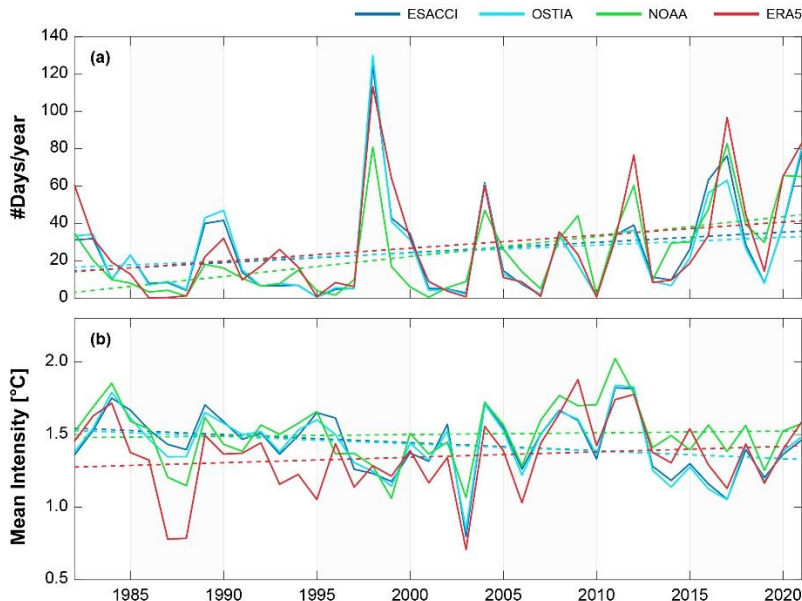
170 3.1.2 Dataset comparison

Given that the comparative analysis of MHW detection methods yielded similar results for the PS, we focus the following dataset comparison exclusively on this region. We therefore apply the Fixed Baseline approach for MHW detection, as proposed by Hobday et al. (2016). A comparative assessment of MHWs across the four SST datasets considered (ESACCI, OSTIA, NOAA, and ERA5) presents an overall agreement on the frequency, duration, and mean intensity of the MHWs with 175 no significant differences (Table A1). On average, the region experiences 1.9 ± 2 MHWs year⁻¹ with a mean duration of 23.6 to 28 days and intensities of 1.36 ± 0.3 °C.

There are, nonetheless, significant differences when the year-to-year variability is examined. For example, in 1998, the NOAA dataset analysis identified 81 MHW days in the PS (Fig. 4a). In contrast, the ESACCI, OSTIA, and ERA5 datasets yielded notably longer durations, with 124, 130, and 113 MHW days, respectively. The number of MHW days per year depicted from 180 the NOAA database remains consistently lower before 2005, and the intensity is likewise lower (Fig. 4a). In contrast, post-2005 values are comparable to, or even exceed, those from other datasets. These temporal discrepancies result in a markedly higher long-term trend in MHW frequency estimated from the NOAA dataset (10.7 events year⁻¹ decade⁻¹) compared to the



ESACCI dataset ($5.5 \text{ events year}^{-1} \text{ decade}^{-1}$). Nonetheless, despite the difference, neither trend is statistically significant (Fig. 4, Table A2).



185

Figure 4: Dataset comparison for Marine Heatwaves assessment in the PS. (a) Interannual variability of MHWs number of days year $^{-1}$; and (b) Mean interannual intensity. Dotted lines represent the linear trends of MHWs number of days year $^{-1}$ and mean intensity (°C) by dataset (see Table A2 for statistics).

3.2 Distribution and Trends of MHWs in the PS

190 The distribution of MHW parameters in the PS reveals an average frequency of approximately 1 to 2.5 events per year (Fig. 5a), with a cumulative duration of 20 to 30 days annually (Fig. 5b). The highest occurrence rates ($2.5 \text{ events year}^{-1}$) are observed at northern latitudes, particularly in the northern tip of the study area and the southwestern Buenos Aires Province coast, whereas moderate frequencies ($2.3 \text{ events year}^{-1}$) are found further south, near the Malvinas Islands and the Burdwood Bank. Temperature anomalies typically range between 0.5°C and 2.5°C , with the highest intensities observed along the 195 northern boundary of the study area, the southwestern Buenos Aires Province coast, and along the northern shelf break (Fig. 6c). In contrast, MHWs are weaker ($\sim 1^\circ\text{C}$) across the rest of the PS, particularly along the continental coastline and around the Malvinas Islands.

Trends in the frequency and duration of MHWs in the PS are predominantly positive north of 48°S (Fig. 5d-e). In contrast, no 200 significant trends are detected south of this latitude, except in the southernmost region near Tierra del Fuego, where significant cooling trends are observed. This spatial pattern aligns closely with the SST warming trend in the region (Fig. 1c). MHW trends reveal that their frequency is increasing at a rate of 0.5 to 1.5 events year $^{-1} \text{ decade}^{-1}$, while the MHW duration (days per year) increases by 10 to 20 days decade $^{-1}$ (Fig. 5d-e). Notably, the reduction in MHW activity at the southern tip of the Argentine Shelf coincides an increase in the frequency and duration of Marine Cold Spells (MCSs; Schlegel et al. 2021), which



are intensifying at rates of 0.5 to 1 event per year decade⁻¹ and 5 to 10 days year⁻¹ decade⁻¹, respectively (Fig. B1). Overall, 205 MHW intensity across the PS shows a slight decline of approximately -0.2 °C.

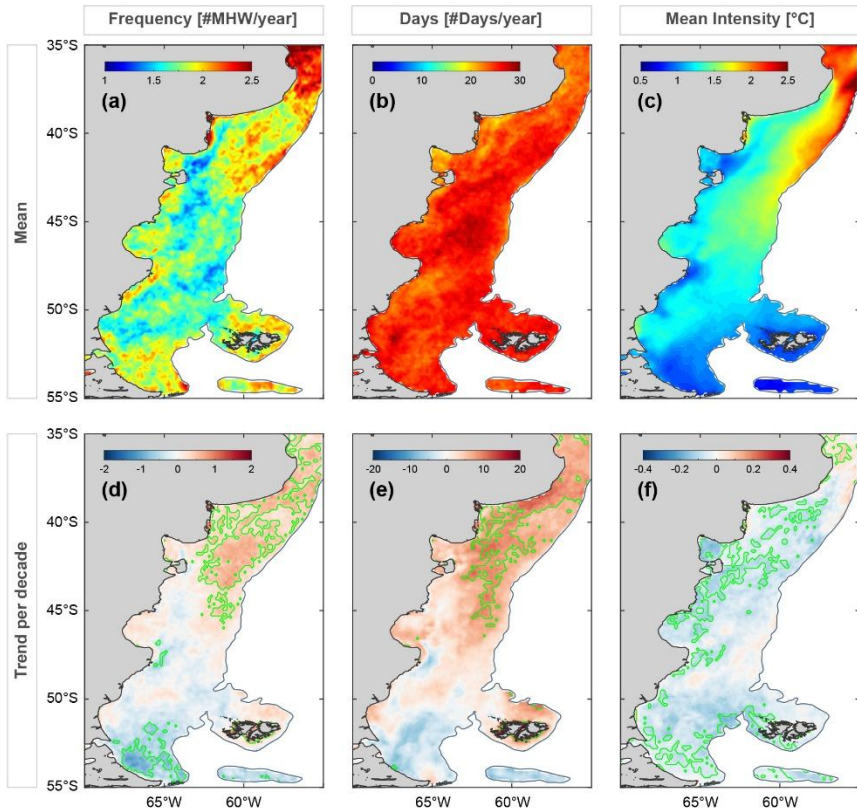


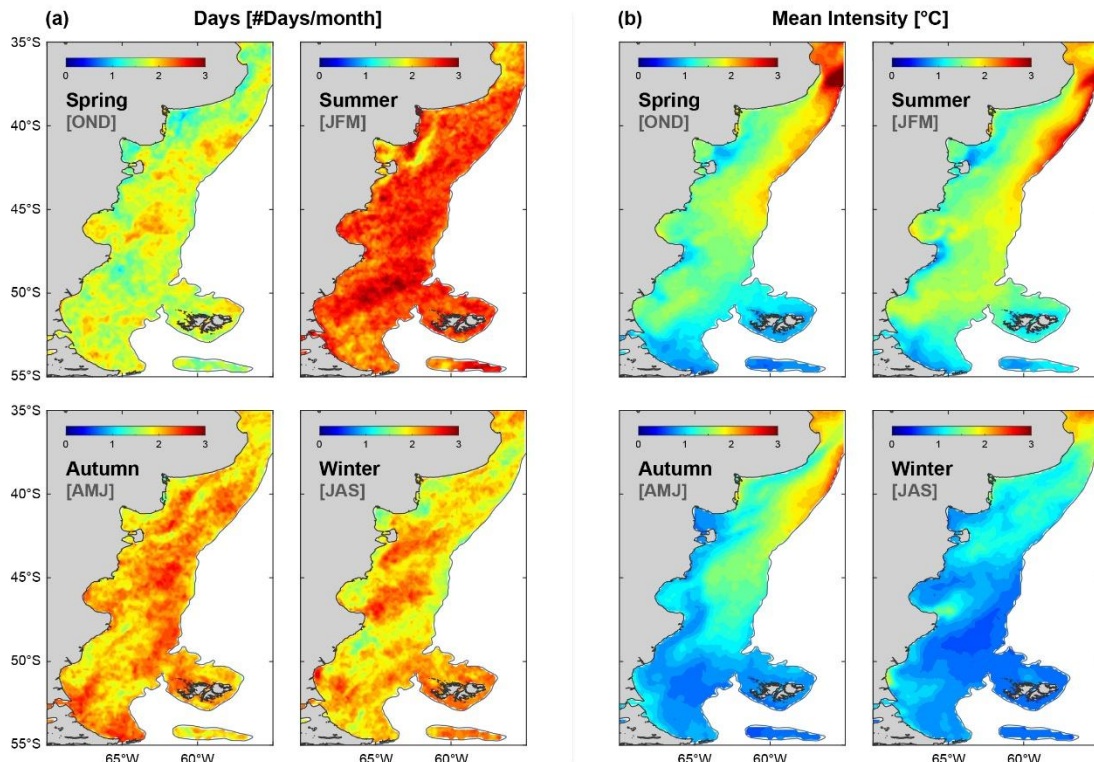
Figure 5: Marine Heatwaves in the Patagonian Continental Shelf. Mean frequency (a), number of MHW days (b), and intensity (c); trends per decade are shown in (d), (e) and (f). Areas in green are statistically significant ($p < 0.05$).

3.3 Seasonality of MHWs in the PS

210 The number of MHW days in the PS exhibits pronounced seasonality (Fig. 6). The austral spring registers the lowest number of MHW activity, averaging approximately 1.8 days month⁻¹. In contrast, MHW occurrence increases notably during summer, and to a lesser extent in autumn, with summer months exhibiting a ~40% increase in MHW days relative to spring. 215 Elevated MHW intensities exceeding 2.5°C are primarily observed during austral spring and summer, particularly in the northern shelf break region and near the Río de la Plata (Fig. 6b). In autumn and winter, MHWs rarely reach 1.5°C, especially within the mid-shelf domain. As noted by Wang and Zhou (2004), air-sea heat fluxes play a pivotal role in modulating cumulative MHW intensity during the warmer seasons, as they integrate both the event duration and the thermal magnitude. Temporal trends in MHWs also display marked seasonal variability, with the most substantial changes observed in event duration rather than intensity (Fig. B2). Notably, across much of the Patagonian Shelf, MHW duration exhibits stronger positive trends during autumn and winter, with increases of up to 2 additional days month/decade. These seasonal extensions



220 are particularly significant for assessing some ecological impacts, such as the effect of MHWs on secondary phytoplankton blooms, which typically occur in late autumn and have been reported to increase in frequency in recent years (Delgado et al., 2023).



225 **Figure 6: Seasonal behaviour of MHW. (a) average number of MHW days month⁻¹ for each season; (b) Average intensity in °C per season.**

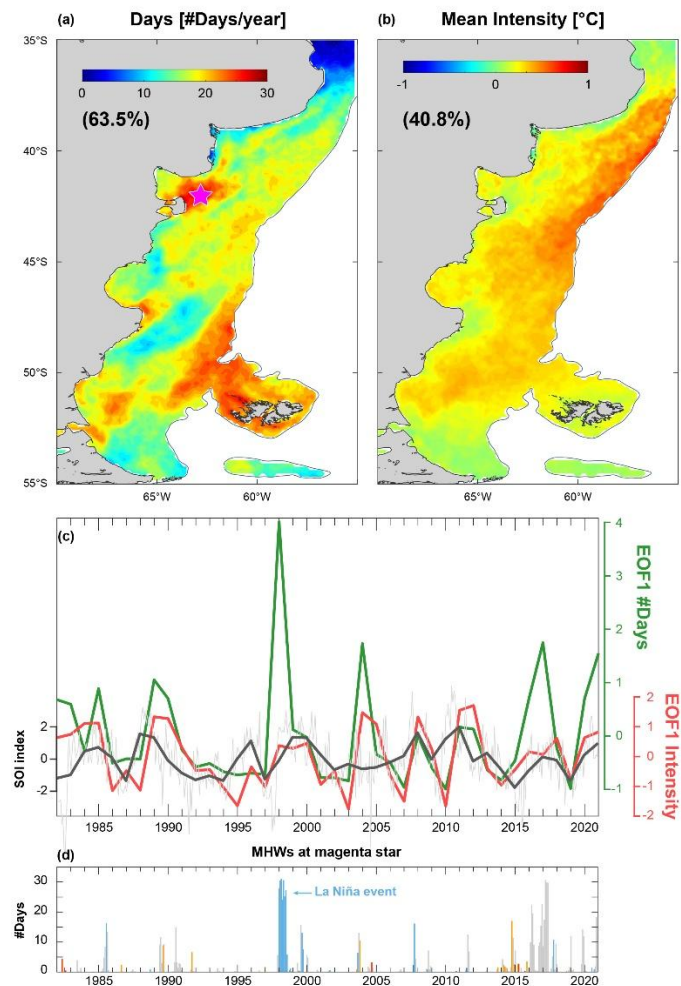
3.4 Interannual variability of MHWs

The leading empirical orthogonal function mode (EOF1) of the number of MHW days year⁻¹ and mean MHW intensity account for 63.5% and 40.8% of the total variance, respectively (Fig. 7a-b). Both exhibit pronounced interannual variability and are significantly correlated ($r = 0.57$; $p < 0.05$). While correlated in time, their corresponding spatial patterns differ in the location 230 of maximum variability. For instance, the northern sector of the shelf break displays greater variability in MHW intensity than in duration, with temperature anomalies during extreme events reaching up to 1.5°C above the mean MHW intensity. Certain shelf regions appear especially susceptible to prolonged MHWs, including the inner and mid-shelf areas off Peninsula Valdés, the vicinity of the Malvinas Islands, and the southern Santa Cruz mid-shelf. In these locations, extreme events have been recorded with durations extended by 30 to 110 days relative to average conditions during peak years. This suggests regionally 235 distinct drivers and responses in MHW characteristics, even within coherent large-scale modes.



240

Except for the 1998 La Niña event, peaks in MHW duration generally coincide with transitions from El Niño to La Niña conditions, marked by shifts from negative to positive values of the Southern Oscillation Index (SOI). In contrast, MHW intensity tends to remain elevated during prolonged positive SOI phases. Although the correlation between the first empirical orthogonal function (EOF-1) of MHW intensity and SOI is weak ($r = 0.14, p < 0.05$), a consistent pattern emerges linking variability in intensity and the number of MHW days to SOI fluctuations. This observation aligns with the findings of Artana et al. (2024), who reported a strong association between MHW duration and intensity in the southwestern Atlantic and the positive phase of SOI, characteristic of La Niña conditions.



245

Figure 7: Spatial patterns of the first EOF modes of the interannual variability in (a) number of days, and (b) mean intensity and (c) the corresponding time series of expansion coefficients overlayed on monthly (grey) and annual mean (black) SOI index. El Niño (La Niña) phases correspond to negative (positive) SOI indexes. (d) Time series of MHW events at a shelf location in the Península Valdés front, as indicated by the magenta star in Fig. 7a.



250

4 Summary and future perspectives

Ecological and societal impacts of MHWs are an issue of increasing concern. While the consequences of the most intense warming events have well-documented effects across entire marine foodwebs (Samhouri et al, 2021; Suryan et al., 2021), some ecological impacts may arise from the cumulative impact of recurrent events or from prolonged, albeit less intense, thermal anomalies. The present study provides a comprehensive analysis of temperature anomalies reported MHWs in the PS, a highly productive and biologically diverse ocean region. The intensity of MHWs in this region (0.5-2.5 °C) is in the range the values reported for other world regions (Wang et al., 2024); however, a positive trend in the northern PS in their duration is evidenced (10-20 days/decade) suggesting persistency rather than intensity may eventually become a major environmental problem.

260 In general, the definition of extreme events remains a critical issue for ensuring consistency in research and for facilitating effective communication among marine scientists, policymakers, and the public (Smith et al., 2025). The detection and characterization of MHWs are particularly sensitive to methodological choices, which can substantially influence their interpretation. In this study, we also compared the outputs of four different SST datasets and two methodological approaches, Fixed and Moving Baseline, across the PS and the SWA. While the mean MHW parameters showed broadly consistent results 265 across datasets and methods, notable discrepancies emerged when analyzing individual events or short-term periods (e.g., spanning only a few years). Methodological differences were most pronounced in the open ocean, where strong SST trends prevail. For instance, over the ZA, where the SST trend exceeds $0.3^{\circ}\text{C decade}^{-1}$, the MHW duration trend reaches 30 days decade^{-1} and is statistically significant when using the MB approach. In contrast, over the Patagonian Shelf, both methodologies 270 yielded comparable results, suggesting that methodological sensitivity is region-specific and influenced by the magnitude of underlying temperature trends.

Within the PS, the highest occurrence of MHWs is observed in the northern sector of the PS, particularly near the La Plata Estuary, where surface temperatures are generally higher (mean 17°C), as well as in specific regions along the continental shelf. The observed increase in MHW duration in the northern PS may be reasonably attributed to shifts in the position of the latitudinal SST gradient characteristic of this area (Fig. 1b). However, the presence of persistent warming hotspots along the 275 coast deserves further analysis. Coastal recirculation patterns and advection anomalies, warming due to riverine outflows, or localized atmospheric processes favoring reduced heat loss from the ocean to the atmosphere may contribute to the formation and maintenance of these anomalies, which can critically affect littoral and intertidal organisms.

Part of the variability of MHW intensity and duration can be attributed to climate variability. Both parameters tend to increase during La Niña episodes, with MHW intensity showing a more consistent association with La Niña conditions. Given the 280 increasing strength of La Niña events (Geng et al., 2023), it is crucial to monitor regions with high interannual variability, especially those showing significant positive trends, such as Península Valdez front and the northern shelf-break front.



Additional mechanisms, including regional atmospheric processes, may also exert a significant influence and should be considered in future analyses of the driving mechanisms.

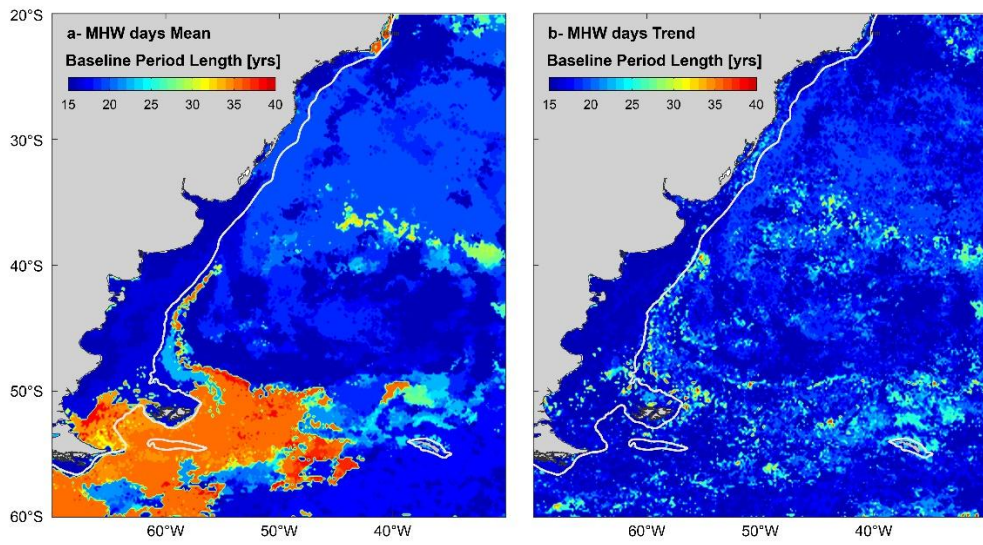
Appendix A: Sensitivity analysis of dataset and length of the baseline period

Dataset	Frequency (#MHW year ⁻¹)	Number of Days (#Days year ⁻¹)	Mean intensity (°C)
ESACCI	1.9 ± 2.0	25.3 ± 33.6	1.36 ± 0.30
OSTIA	1.9 ± 2.0	24.8 ± 33.3	1.36 ± 0.30
NOAA	2.0 ± 2.1	23.6 ± 30.5	1.44 ± 0.28
ERA5	2.1 ± 2.2	28.0 ± 37.9	1.31 ± 0.25

285 **Table A1. Marine Heat Waves Statistics. Mean and standard deviation (from yearly time series) values are computed for the Patagonian Shelf.**

Dataset	Slope (#Days year ⁻¹)	Slope (mean intensity °C year ⁻¹)
ESACCI	0.5 ± 0.7	-0.0055 ± 0.0058
OSTIA	0.4 ± 0.7	-0.0051 ± 0.0058
NOAA	1.0 ± 0.5	0.0012 ± 0.0058
ERA5	0.6 ± 0.7	0.0037 ± 0.0072

Table A2. Marine Heat Waves dataset trends statistics for the Patagonian Shelf. In bold, statistically significant (95% confidence).

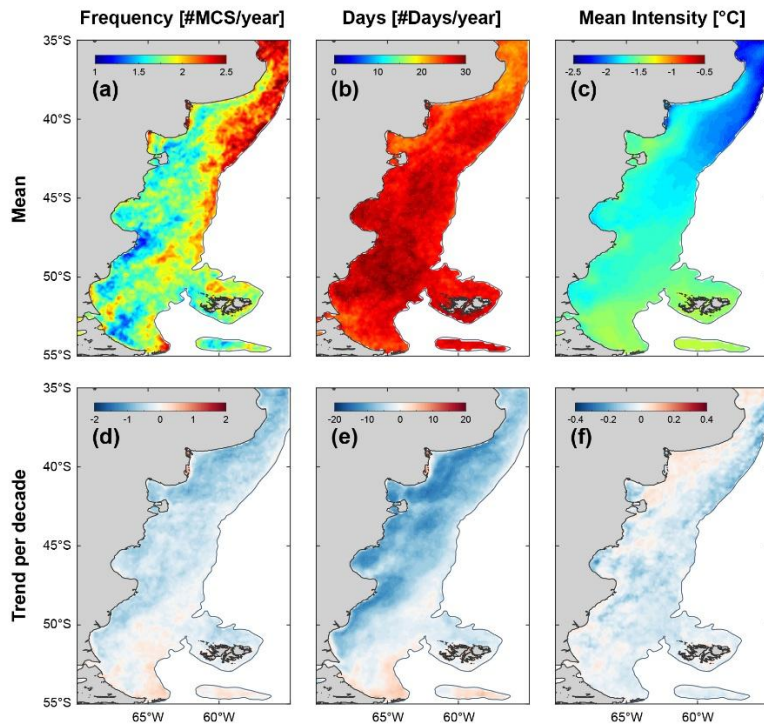


290

Figure A1. Length of the Baseline period [in years], when the 1982-2021 mean (a) and trend (b) MHWs days is maximum.



Appendix B: Marine Cold Spells in the Patagonian Shelf



295 **Figure B1. Marine Cold Spells in the Patagonian Continental Shelf. Mean frequency (a), number of days (b), intensity (c); trend per decade of frequency (d), number of days (e), intensity (f).**

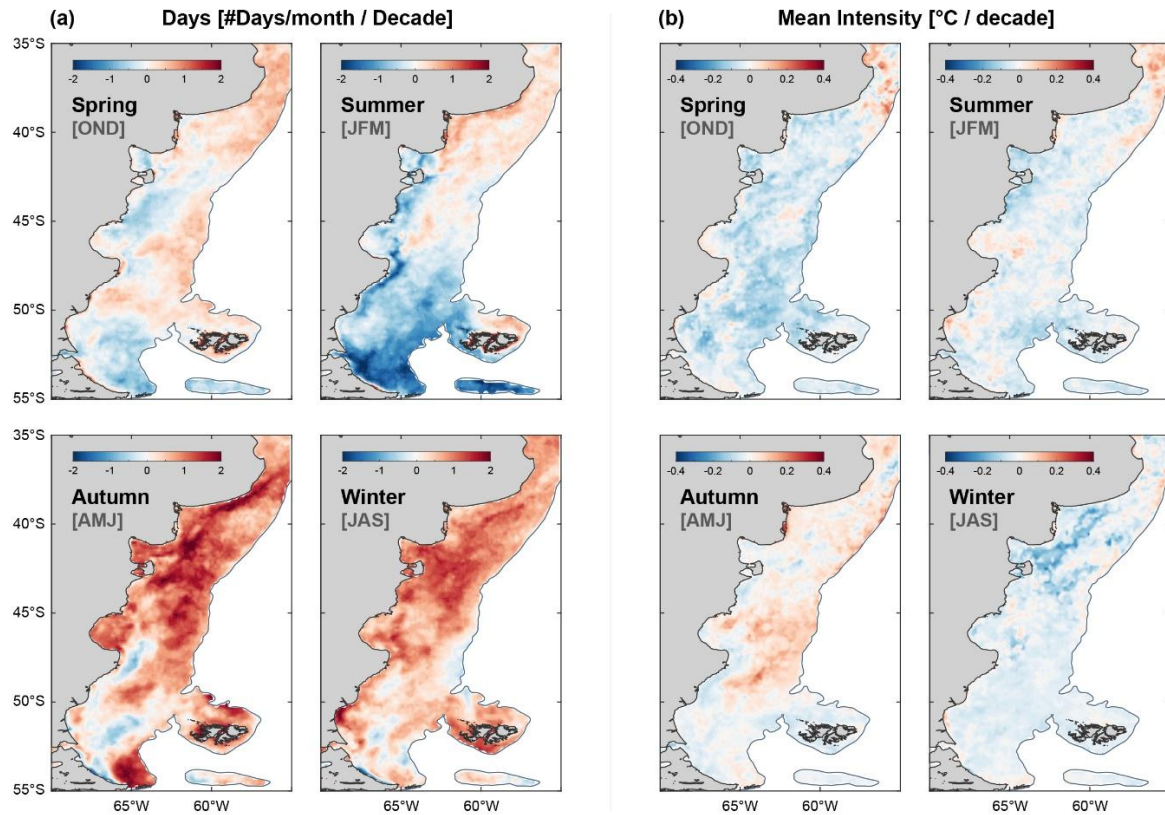


Figure B2. Seasonal Marine Heatwaves trends in number of days month⁻¹ decade⁻¹ and mean intensity (°C decade⁻¹).

Data availability

300 All raw data can be provided by the corresponding authors upon request.

Author contributions

ALD and VC conceptualized the manuscript. VC performed the data curation and developed the methodology. ALD and VC conducted the formal analysis. ALD and GB acquired the funding. ALD wrote the original draft. ALD, VC and GB reviewed and edited the manuscript.

305 Competing interests

The authors declare that they have no conflict of interest.



Financial support

The present research was carried out within the framework of the activities of the Spanish Government through the “María de Maeztu Centre of Excellence” accreditation to IMEDEA (CSIC-UIB) (CEX2021-001198-M). A.L.D. acknowledges funding

310 by an individual postdoctoral fellowship “Vicenç Mut” (PD/002/2022) from Govern de les Illes Balears and Fondo Social Europeo and the Consejo Nacional de Investigaciones Científicas y Técnicas (CONICET). V.C. acknowledges the support from the Spanish Ramón y Cajal Program (RYC2020-029306-I) through Grant AEI/UIB—10.13039/501100011033.

References

Artana, C., Provost, C., Lellouche, J. M., Rio, M. H., Ferrari, R., and Sennéchal, N.: The Malvinas current at the confluence with the Brazil current: Inferences from 25 years of Mercator ocean reanalysis, *J. Geophys. Res. Oceans*, 124(10), 7178–7200, <https://doi.org/10.1029/2019JC015289>, 2019.

Artana, C., Rodrigues, R. R., Fevrier, J., and Coll, M.: Characteristics and drivers of marine heatwaves in the western South Atlantic, *Commun. Earth Environ.*, 5(1), 555, <https://doi.org/10.1038/s43247-024-01726-8>, 2024.

Boisséson, E. and Balmaseda, M. A.: Predictability of marine heatwaves: assessment based on the ECMWF seasonal forecast system, *Ocean Sci.*, 20, 265–278, <https://doi.org/10.5194/os-20-265-2024>, 2024.

Brauko, K. M., Cabral, A., Costa, N. V., Hayden, J., Dias, C. E., Leite, E. S., ... and Horta, P. A.: Marine heatwaves, sewage and eutrophication combine to trigger deoxygenation and biodiversity loss: a SW Atlantic case study, *Front. Mar. Sci.*, 7, 590258, <https://doi.org/10.3389/fmars.2020.590258>, 2020.

Cai, W., McPhaden, M. J., Grimm, A. M., Rodrigues, R. R., Taschetto, A. S., Garreaud, R. D., ... and Vera, C.: Climate impacts of the El Niño–southern oscillation on South America. *Nat. Rev. Earth Environ.*, 1(4), 215–231., <https://doi.org/10.1038/s43017-020-0040-3>, 2020.

Carvalho, K. S., Smith, T. E., and Wang, S.: Bering Sea marine heatwaves: Patterns, trends and connections with the Arctic, *J. Hydrol.*, 600, 126462, <https://doi.org/10.1016/j.jhydrol.2021.126462>, 2021.

Cavole, L. M., Demko, A. M., Diner, R. E., Giddings, A., Koester, I., Pagniello, C. M. L. S., et al.: Biological impacts of the 2013–2015 warm-water anomaly in the Northeast Pacific: winners, losers, and the future, *Oceanogr.*, 29, 273–285, <https://doi.org/10.5670/oceanog.2016.32>, 2016.

Cheung, W. W., and Frölicher, T. L.: Marine heatwaves exacerbate climate change impacts for fisheries in the northeast Pacific, *Sci. Rep.*, 10(1), 6678, <https://doi.org/10.1038/s41598-020-63650-z>, 2020.

Dai, A., Trenberth, K.E.: Estimates of freshwater discharge from continents: latitudinal and seasonal variations, *J. Hydrometeorol.* 3, 660–687, [https://doi.org/10.1175/1525-7541\(2002\)003<0660:EOFDFC>2.0.CO;2](https://doi.org/10.1175/1525-7541(2002)003<0660:EOFDFC>2.0.CO;2), 2002.

Delgado, A. L., Hernández-Carrasco, I., Combes, V., Font-Muñoz, J., Pratolongo, P. D., and Basterretxea, G.: Patterns and trends in chlorophyll-a concentration and phytoplankton phenology in the biogeographical regions of Southwestern Atlantic, *J. Geophys. Res. Oceans.*, 128(9), e2023JC019865, <https://doi.org/10.1029/2023JC019865>, 2023.



Embry, O., Merchant, C.J., Good, S.A. et al.: Satellite-based time-series of sea-surface temperature since 1980 for climate 340 applications, *Sci. Data.*, 11, 326, <https://doi.org/10.1038/s41597-024-03147-w>, 2024.

FAO: The State of Food and Agriculture 2020. Overcoming water challenges in agriculture, Food and Agriculture Organization of the United Nations, <https://doi.org/10.4060/cb1447en>, 2020.

Franco, B. C., Combes, V., and González Carman, V.: Subsurface ocean warming hotspots and potential impacts on marine 345 species: the southwest South Atlantic Ocean case study, *Front. Mar. Sci.*, 7, 563394, <https://doi.org/10.3389/fmars.2020.563394>, 2020.

Frölicher, T. L., Fischer, E. M. and Gruber, N.: Marine heatwaves under global warming, *Nat.*, 560, 360–364, <https://doi.org/10.1038/s41586-018-0383-9>, 2018.

Genevier, L. G. C., T. Jamil, D. E. Raitsos, G. Krokos, and I. Hoteit: Marine heatwaves reveal coral reef zones susceptible to 350 bleaching in the Red Sea, *Glob. Chang. Biol.*, 25, 2338–2351, <https://doi.org/10.1111/gcb.14652>, 2019.

Geng, T., Jia, F., Cai, W., Wu, L., Gan, B., Jing, Z., ... and McPhaden, M. J.: Increased occurrences of consecutive La Niña 355 events under global warming, *Nat.*, 619(7971), 774-781, <https://doi.org/10.1038/s41586-023-06236-9>, 2023.

Good, S., Fiedler, E., Mao, C., Martin, M.J., Maycock, A., Reid, R., Roberts-Jones, J., Searle, T., Waters, J., While, J., Worsfold, M.: The Current Configuration of the OSTIA System for Operational Production of Foundation Sea Surface 360 Temperature and Ice Concentration Analyses, *Remote Sens.*, 12, 720, <https://doi.org/10.3390/rs12040720>, 2020.

Gordon, A. L.: Brazil-malvinas confluence–1984, *Deep-Sea Res. I*, 36(3), 359-384, [https://doi.org/10.1016/0198-0149\(89\)90042-3](https://doi.org/10.1016/0198-365 0149(89)90042-3), 1989.

Gordon, A. L., and Greengrove, C. L.: Geostrophic circulation of the Brazil-Falkland confluence, *Deep-Sea Res. I*, 33(5), 573– 370 585, [https://doi.org/10.1016/0198-0149\(86\)90054-3](https://doi.org/10.1016/0198-0149(86)90054-3), 1986.

Gregory, C. H., Artana, C., Lama, S., León-FonFay, D., Sala, J., Xiao, F., and Holbrook, N. J., Global marine heatwaves under 360 different flavors of ENSO, *Geophys. Res. Lett.*, 51(20), e2024GL110399, <https://doi.org/10.1029/2024GL110399>, 2024.

Hersbach, H., Bell, B., Berrisford, P., Biavati, G., Horányi, A., Muñoz Sabater, J., Nicolas, J., Peubey, C., Radu, R., Rozum, I., Schepers, D., Simmons, A., Soci, C., Dee, D., Thépaut, J-N.: ERA5 hourly data on single levels from 1940 to present, Copernicus Climate Change Service (C3S) Climate Data Store (CDS), <https://doi.org/10.24381/cds.adbb2d47>, 2023.

Heidemann, H., and Ribbe, J.: Marine heat waves and the influence of El Niño off Southeast Queensland, Australia, *Front. 365 Mar. Sci.*, 6, 56, <https://doi.org/10.3389/fmars.2019.00056>, 2019.

Hobday, A. J., and Pecl, G. T.: Identification of global marine hotspots: sentinels for change and vanguards for adaptation 370 action, *Rev. Fish Biol. Fish.*, 24, 415-425, <https://doi.org/10.1007/s11160-013-9326-6>, 2014.

Holbrook, N. J., Scannell, H. A., Sen Gupta, A., Benthuyzen, J. A., Feng, M., Oliver, E. C., ... and Wernberg, T.: A global 370 assessment of marine heatwaves and their drivers, *Nat. Commun.*, 10(1), 2624, <https://doi.org/10.1038/s41467-019-10206-z>, 2019.

Hu, S., Zhang, L., and Qian, S.: Marine heatwaves in the Arctic region: Variation in different ice covers, *Geophys. Res. Lett.*, 47(16), e2020GL089329, <https://doi.org/10.1029/2020GL089329>, 2020.



Huang, B., C. Liu, V. Banzon, E. Freeman, G. Graham, B. Hankins, T. Smith, and H.-M. Zhang: Improvements of the Daily Optimum Interpolation Sea Surface Temperature (DOISST) Version 2.1, *J. Clim.*, 34, 2923-2939, 375 <https://doi.org/10.1175/JCLI-D-20-0166.1>, 2021.

IPCC, 2021: Climate Change 2021: The Physical Science Basis. Contribution of Working Group I to the Sixth Assessment Report of the Intergovernmental Panel on Climate Change [Masson-Delmotte, V., P. Zhai, A. Pirani, S.L. Connors, C. Péan, S. Berger, N. Caud, Y. Chen, L. Goldfarb, M.I. Gomis, M. Huang, K. Leitzell, E. Lonnoy, J.B.R. Matthews, T.K. Maycock, T. Waterfield, O. Yelekçi, R. Yu, and B. Zhou (eds.)]. Cambridge University Press, Cambridge, United Kingdom and New York, NY, USA, 2391 pp. doi:10.1017/9781009157896.

Kitchel, Z. J., Conrad, H. M., Selden, R. L., and Pinsky, M. L.: The role of continental shelf bathymetry in shaping marine range shifts in the face of climate change, *Global Change Biol.*, 28(17), 5185-5199, <https://doi.org/10.1111/gcb.16276>, 2022.

Konsta, K., Doxa, A., Katsanevakis, S. et al.: Projected marine heatwaves over the Mediterranean Sea and the network of marine protected areas: a three-dimensional assessment, *Clim. Change.*, 178, 17, <https://doi.org/10.1007/s10584-025-03860-4>, 2025.

Liu, K., Xu, K., Zhu, C., and Liu, B.: Diversity of marine heatwaves in the South China Sea regulated by ENSO phase, *J. Clim.*, 35(2), 877-893, <https://doi.org/10.1175/JCLI-D-21-0309.1>, 2022.

Matano, R. P., and Philander, S. G. H.: Heat and mass balances of the South Atlantic Ocean calculated from a numerical model, *J. Geophys. Res.*, 98, 977-984, <https://doi.org/10.1029/92jc01899>, 1993.

390 Matano, R.P., Palma, E.D., Piola, A.R.: The influence of the Brazil and Malvinas currents on the southwestern Atlantic shelf circulation, *Ocean Sci.*, 6, 983-995, <https://doi.org/10.5194/os-6-983-2010>, 2010.

McPhaden, M. J., Zebiak, S. E., Glantz, M. H.: ENSO as an integrating concept in earth science, *Sci.*, 314(5806), 1740-1745, <https://doi.org/10.1126/science.1132588>, 2006.

Mignot, A., Von Schuckmann, K., Landschützer, P., Gasparin, F., van Gennip, S., Perruche, C., ... and Amm, T.: Decrease in 395 air-sea CO₂ fluxes caused by persistent marine heatwaves, *Nat. Commun.*, 13(1), 4300, <https://doi.org/10.1038/s41467-022-31983-0>, 2022.

Oliver, E. C., BenthuySEN, J. A., Bindoff, N. L., Hobday, A. J., Holbrook, N. J., Mundy, C. N., and Perkins-Kirkpatrick, S. E.: The unprecedented 2015/16 Tasman Sea marine heatwave, *Nat. Commun.*, 8(1), 16101, <https://doi.org/10.1038/ncomms16101>, 2017.

400 Oliver, E.C.J., Donat, M.G., Burrows, M.T. et al. : Longer and more frequent marine heatwaves over the past century, *Nat. Commun.*, 9, 1324, <https://doi.org/10.1038/s41467-018-03732-9>, 2018.

Oliver, E. C. J.: Mean warming not variability drives marine heatwave trends, *Clim. Dyn.*, 53, 1653-1659, <https://doi.org/10.1007/s00382-019-04707-2>, 2019.

Oliver E.C.J., BenthuySEN J.A., Darmaraki S., Donat M.G., Hobday A.J., Holbrook N.J., Schlegel R.W., Sen Gupta A.: Marine 405 Heatwaves, *Ann. Rev. Mar. Sci.*, 13, 313-342, <https://doi.org/10.1146/annurev-marine-032720-095144>, 2021.



Olson, D. B., Podestá, G. P., Evans, R. H., and Brown, O. B.: Temporal variations in the separation of Brazil and Malvinas Currents, Deep-Sea Res. I, 35, 1971–1990, [https://doi.org/10.1016/0198-0149\(88\)90120-3](https://doi.org/10.1016/0198-0149(88)90120-3), 1988.

Palma, E.D., Matano, R.P., Piola, A.R.: A numerical study of the Southwestern Atlantic Shelf circulation: barotropic response to tidal and wind forcing, J. Geophy. Res. Oceans, 109, C08014, <https://doi.org/10.1029/2004JC002315>, 2004.

410 Risaro, D. B., Chidichimo, M. P., and Piola, A. R.: Interannual variability and trends of sea surface temperature around southern South America, Front. Mar. Sci., 9, 829144, <https://doi.org/10.3389/fmars.2022.829144>, 2022.

Rivas, A.L.: Current-meter observations in the Argentine continental shelf, Continent. Shelf Res. 17, 391–406, [https://doi.org/10.1016/S0278-4343\(96\)00039-8](https://doi.org/10.1016/S0278-4343(96)00039-8), 1997.

415 Rosselló, P., Pascual, A., and Combes, V.: Assessing marine heat waves in the Mediterranean Sea: a comparison of fixed and moving baseline methods, Front. Mar. Sci., 10, 1168368, <https://doi.org/10.3389/fmars.2023.1168368>, 2023.

Samhouri, J. F., Feist, B. E., Fisher, M. C., Liu, O., Woodman, S. M., Abrahms, B., ... and Saez, L. E.: Marine heatwave challenges solutions to human–wildlife conflict, Proc. R. Soc. Lond. B Biol. Sci., 288(1964), 20211607, <https://doi.org/10.1098/rspb.2021.1607>, 2021.

420 Schlegel, R. W., Darmaraki, S., Benthuyzen, J. A., Filbee-Dexter, K., and Oliver, E. C.: Marine cold-spells, Prog. Oceanogr., 198, 102684, <https://doi.org/10.1016/j.pocean.2021.102684>, 2021.

Smale, D.A. et al.: Marine heatwaves threaten global biodiversity and the provision of ecosystem services, Nat. Clim. Change, 9, 306–312, <https://doi.org/10.1038/s41558-019-0412-1>, 2019.

Smith, K. E., Gupta, A. S., Amaya, D., et al.: Baseline matters: Challenges and implications of different marine heatwave baselines, Prog. Oceanogr., 231, 103404, <https://doi.org/10.1016/j.pocean.2024.103404>, 2025.

425 Stott, P. A., Gillett, N. P., Hegerl, G. C., Karoly, D. J., Stone, D. A., Zhang, X., and Zwiers, F.: Detection and attribution of climate change: a regional perspective, WIREs Clim. Change, 1(2), 192–211, <https://doi.org/10.1002/wcc.34>, 2010.

Suryan, R.M., Arimitsu, M.L., Coletti, H.A. et al.: Ecosystem response persists after a prolonged marine heatwave, Sci. Rep. 11, 6235, <https://doi.org/10.1038/s41598-021-83818-5>, 2021.

430 Wang, Y. and Zhou Y.: Seasonal dynamics of global marine heatwaves over the last four decades, Front. Mar. Sci., 11, 1406416, <https://doi.org/10.3389/fmars.2024.1406416>, 2024.

Webster, P. J., and Palmer, T. N.: The past and the future of El Niño, Nat., 390(6660), 562–564, <https://doi.org/10.1038/37499>, 1997.

Xie, S. P., Deser, C., Vecchi, G. et al.: Towards predictive understanding of regional climate change, Nat. Clim Change 5, 921–930, <https://doi.org/10.1038/nclimate2689>, 2015.

435